

# Thin Self-Resonant Structures with a High- $Q$ for Wireless Power Transfer

Aaron L.F. Stein      Phyo Aung Kyaw      Jesse Feldman-Stein      Charles R. Sullivan  
Thayer School of Engineering, Dartmouth College, Hanover, NH 03755 USA  
Email: {Aaron.L.Stein, Phyo.A.Kyaw.TH, Jesse.C.Feldman-Stein.18, Charles.R.Sullivan}@dartmouth.edu

**Abstract**—The range, efficiency, and size of resonant coils in an inductive wireless charging system is determined by the quality factor  $Q$  of the resonant coils. The multi-layer self-resonant structure is a new resonant coil technology that has been demonstrated to have a  $Q$   $6\times$  larger than conventional coils. However, to date, implementations of this structure have been thick, which limits their practical applications. In this paper, we explore the relationship between the thickness of a self-resonant structure and its performance. A computationally efficient 2-D optimization algorithm is proposed to design thin resonant structures and illustrate the trade-offs in the design. A new magnetic core shape is proposed which shapes the magnetic field lines to be parallel to the conductive layers and reduces current crowding. Finally, a prototype 3.5 mm thick self-resonant structure is constructed, which has a measured quality factor of 560 despite having a diameter of only 6.6 cm; this provides a  $3.03\times$  improvement over the state-of-the-art wireless power transfer coils in the literature.

## I. INTRODUCTION

Resonant inductive wireless power transfer (WPT) provides a convenient and safe method for powering and recharging mobile electronic devices. The effectiveness of WPT is determined by the efficiency and range of the power transfer, which are limited by the quality factor  $Q$  and magnetic coupling factor  $k$  of the resonant coils. As the distance between resonant coils increases, the magnetic coupling factor decreases, and therefore increasing  $Q$  is essential for increasing the range and efficiency of WPT [1]. Furthermore, in many mobile electronic devices it is difficult to remove heat from the resonant coils, which makes the  $Q$  of the coil an important parameter in order to maintain safe operating temperatures.

The achievable quality factor of resonant coils depends on the diameter of the coil [2]. So, a figure-of-merit  $Q_d$  is proposed in [1], which is the quality factor normalized by diameter  $d$ . Conventional coils, made of solid or litz wire, have a  $Q_d$  ranging from 3 to  $28\text{ cm}^{-1}$  [3]–[8].

In the MHz frequency range, only a small portion of solid wire can be utilized due to skin effect, and proximity loss in litz wire at MHz frequencies is very high because strand diameters are too large compared to the skin depth  $\delta$ . Thinner strands would reduce this loss, but are very difficult to manufacture [9].

The self-resonant structure, described in detail in [1], [10], overcomes many of the issues associated with conventional resonant coils. It is an integrated LC resonator constructed from alternating C-shaped thin conductive layers and washer-shaped dielectric layers that are stacked into a magnetic core.

This structure can achieve a very high  $Q$  because it forces equal current sharing between many thin layers, has no terminations in the resonant current path, and orients conductive materials parallel to the magnetic field. In [1], a prototype of this structure was shown to have a quality factor of 1173 despite having a diameter of only 6.6 cm. The experimental  $Q_d$  of the prototype ( $177\text{ cm}^{-1}$ ) is more than six times that of other coils presented in the literature, which demonstrates the significant performance benefit this technology provides.

The prototype of the self-resonant structure developed in [1] uses a thick magnetic pot core (16.2 mm), which provides many performance benefits but also makes it difficult to integrate in mobile electronic devices. First, the thick core shapes the magnetic field lines to be parallel to the thin conductors, which minimizes eddy current losses. Next, the effective area of the magnetic core can be chosen to minimize core loss. Finally, the thick core shape provides ample space for the winding, which allows the number of layers to be chosen based solely on minimizing winding loss, and allows the use of relatively thick substrates to support the thin foil layer. Although the thick substrates are useful for handling the thin conductor layers, they do not contribute to the performance of the structure and increase the total height of the structure [1].

In this paper, we analyze the relationship between the height and  $Q$  of self-resonant structures (Section II), and use this analysis to develop a methodology for designing thin structures. In Section III, we present a 2-dimensional optimization space which maximizes  $Q$  by allocating space between winding, core, and air space. In Section IV, we introduce a new magnetic core shape, called the modified pot core, that shapes the magnetic field lines in a thin self-resonant structure in order to reduce eddy currents. Finally, in Section V, we use the optimization algorithm, and the new modified pot core in the design of a thin self-resonant structure. Experimental results show that the thin structure has a  $Q$  of 560 and  $Q_d$  of 84.8, which is  $3.03\times$  larger than the current state-of-the-art coils despite having a thickness of only 3.5 mm.

## II. THE CHALLENGE OF HIGH- $Q$ AND THIN SELF-RESONANT STRUCTURES

The self-resonant structure, which is introduced in [1], [10], is a parallel resonator that is constructed from alternating C-shaped thin conductive layers and washer-shaped dielectric layers that are stacked into a magnetic core (see Fig. 1). A

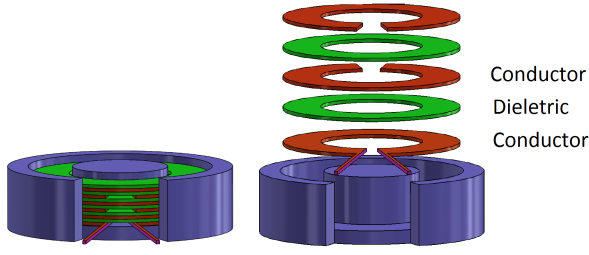


Fig. 1: Self-resonant structure, shown with exaggerated layer thickness for clarity. In practice, layer thicknesses is on the order of 10  $\mu\text{m}$  and many layers are used.

section is two C-shaped foil layers separated by a low-loss dielectric (Fig. 1). The C-shaped conductors within a section have opposite orientations, which results in two overlapping areas and form two capacitors. As current flows through a section it passes through both capacitors, and creates an inductive current loop. This results in a parallel LC resonator in which the inductance  $L$  is equivalent to a single turn around the magnetic core and the capacitance is the series combination of two section-half capacitances  $C_{sh}$  [10]. This section-half capacitance can be expressed in terms of the angle of overlap of the layers in radians  $\theta$ , the inner radius of the coil  $r_1$ , the outer radius  $r_2$ , the permittivity of the dielectric  $\epsilon_d$ , and the dielectric thickness  $t_d$

$$C_{sh} = \epsilon_d \left( \frac{\theta}{2\pi} \right) \left( \frac{\pi (r_2^2 - r_1^2)}{t_d} \right) = \frac{\epsilon_d \theta (r_2^2 - r_1^2)}{2t_d}. \quad (1)$$

The self-resonant structure is constructed from many sections that are separated from each other by a low-loss dielectric layer. Excluding the first layer, each section is inductively coupled so there are no terminations in the resonating high-current path. The strong coupling effectively puts all of the sections in parallel. Each section-half has a capacitance  $C_{sh}$ , and there is additional capacitance between a section and the layers above and below it. Therefore, a structure with  $m$  sections has an equivalent capacitance  $C_{equiv}$  of

$$C_{equiv} = mC_{sh}, \quad (2)$$

and a resonant frequency

$$\omega_0 = \frac{1}{\sqrt{LC_{equiv}}}. \quad (3)$$

The  $Q$  of a self-resonant structure is

$$Q = \frac{\omega_0 L}{R_{total}}, \quad (4)$$

where  $\omega_0$  is the angular resonant frequency and  $R_{total}$  is the equivalent series resistance of the resonant current path; therefore, the impact of structure height  $h_s$  on  $Q$  can be understood by investigating the impact of structure height on  $R_{total}$ . As shown in Fig. 2, the total height of a self resonant structure  $h_s$  limits the space that can be allocated to the height of the winding  $h_w$ , the height of the back-plate of the magnetic core  $h_{bp}$ , and the height of the air gap between the top of

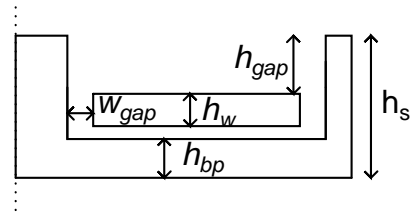


Fig. 2: An axisymmetric diagram of a self resonant structure. This diagram is not to scale, but enlarged in order to clearly define: the winding height  $h_w$ , the magnetic core back-plate height  $h_{bp}$ , and the total height of the structure  $h_s$ .

the winding and the top of the magnetic core  $h_{gap}$ . Limiting these parameters impacts the loss models, developed in [1], [10], which describe  $R_{total}$  as the sum of 3 equivalent series resistances (ESR) that model winding loss  $R_{wind}$ , core loss  $R_{core}$ , and dielectric loss  $R_{dielectric}$ .

#### A. Impact of Thin Structures on Dielectric Loss

The ESR that models dielectric loss  $R_{dielectric}$  is independent of structure thickness, and is

$$R_{dielectric} = \frac{D_d}{C_{equiv}\omega_0}, \quad (5)$$

where  $D_d$  is the dissipation factor of the dielectric material, and  $C_{equiv}$  is the equivalent capacitance of the structure. Substituting (5) into (4) yields

$$Q = \frac{1}{D_d + (R_{core} + R_{winding})\omega_0 C_{equiv}}. \quad (6)$$

This shows the dielectric loss is independent of structure thickness: the effect of  $D_d$  on  $Q$  is independent of structure parameters  $L$  and  $C_{equiv}$ .

#### B. Impact of Thin Structures on Winding Loss

The ESR that models winding loss  $R_{wind}$  increases as the height of the structure decreases.  $R_{wind}$  is modeled in [1], [10] in terms of the thickness of the foil layers  $t_c$ , the coil inner radius  $r_1$  and outer radius  $r_2$  of the winding, the resistivity of the conductor  $\rho$ , the current crowding factor  $F_{cc}$ , and the field weakening factor  $F_{fw}$  as

$$R_{wind} \approx \frac{2\pi\rho}{\ln\left(\frac{r_2}{r_1}\right)t_c m} \left[ k_1 F_{cc} + \frac{F_{fw} m^2}{9} \left( \frac{t_c}{\delta} \right)^4 k_2 \right], \quad (7)$$

where

$$k_1 = 1 - \frac{\theta}{3\pi} \quad \text{and} \quad k_2 = 1 + \frac{\theta}{\pi}. \quad (8)$$

The ESR that models winding resistance is impacted by structure height for two reasons. First, the height of the structure limits the height of the winding  $h_w$ , and restricts the possible winding designs. If  $h_s$  is large, then a large number of sections constructed from conductors much thinner than the skin depth ( $t_c \ll \delta$ ) can be used to minimize (7) without a constraint on the available winding height. However, in the design of thin structures, the height of the winding is limited, which reduces the design space and potentially increases  $R_{wind}$ .

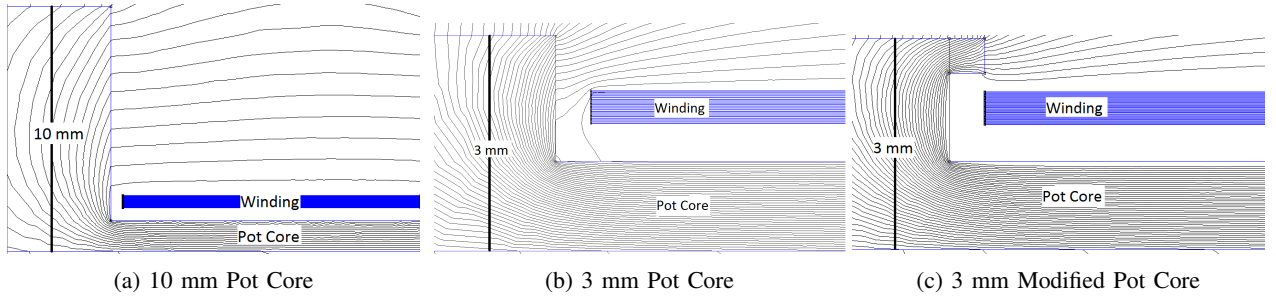


Fig. 3: An axissymmetric finite element analysis is used to show the magnetic field lines on 3 pot cores filled with 10 sections. Each pot core has an  $h_{bp}$  of 1.25 mm but in (a)  $h_s$  is 10 mm and in (b) and (c)  $h_s$  is 3 mm. In (a) the field lines are relatively parallel to the windings due to the height of the core, but with a shorter pot core in (b) it is clear that the field lines are no longer parallel to the foil, and are therefore causing additional eddy currents. To overcome this issue, in Section IV we propose the modified pot core, shown in (c), that straightens the field lines around the winding despite the thin pot core.

Second, the distance between the top of the winding and the top of the magnetic core  $h_{gap}$  has a significant impact on the winding loss, and this space is limited in a thin structure. In Fig. 3a, the large  $h_{gap}$  ensures that the magnetic field lines are mostly parallel to the foil layers, so eddy current losses are small due to the thin layers. In Fig. 3b,  $h_{gap}$  is small and the magnetic field lines are not parallel to the thin conductive layers, which causes eddy currents that result in current crowding near the edge of the conductors and increased winding loss. Therefore,  $h_{gap}$  impacts the  $Q$ . This phenomenon is captured in (7) by  $F_{cc}$ , which is a factor that describes the impact of horizontal current crowding on  $R_{wind}$ .

### C. Impact of Thin Structures on Core Loss

The ESR that models core loss  $R_{core}$  increases as the structure height decreases. For a given core material with a relative permeability of  $\mu' - j\mu''$ ,  $R_{core}$  is

$$R_{core} = \frac{\omega_0 \left( \frac{\ell_{eh}}{\mu_0 A_e} \right) \mu''}{\left( \left( \frac{\ell_{eh}}{\mu_0 A_e} \right) + \mathcal{R}_a \mu' \right)^2 + (\mathcal{R}_a \mu'')^2}, \quad (9)$$

where  $\ell_{eh}$ ,  $A_e$ , and  $\mathcal{R}_a$  are the effective length of the pot core half, the effective area of the core, and the reluctance of the air respectively [1]. In a thin structure, the height of the backplate of the magnetic pot core  $h_{bp}$  is limited, which decreases the effective core area  $A_e$ . At the same time, the effective magnetic length of the pot core half is decreased; however, the reduction in the effective core length is small in comparison to the reduction in effective core area. Therefore, reducing the height of the structure  $h_s$  increases (9).

### III. HEIGHT-CONSTRAINED OPTIMIZATION

The performance of a thin self-resonant structure with a specified height can be optimized by allocating the available height among  $h_{bp}$ ,  $h_w$  and  $h_{gap}$  to maximize  $Q \cdot k$ . However, because the effect of these parameters on the quality factor  $Q$  is much more significant than that on the magnetic coupling factor  $k$ , it is sufficient to optimize  $Q$  instead.  $Q$  is optimized by minimizing the sum of the winding loss, core loss and dielectric loss.

The winding loss model, discussed in Section II-B, has two factors  $F_{cc}$  and  $F_{fw}$  that model the effects of current crowding

and field weakening respectively. Due to the complexities of modeling magnetic fields, these factors are computed using finite element analysis (FEA) [1]. In previous self-resonant structure designs  $h_{gap}$  was relatively large, and therefore  $F_{cc}$  and  $F_{fw}$  were not included in the design process as they did not significantly contribute to the overall loss. However, for the design of thin structures these factors must be considered. The FEA required to compute  $F_{cc}$  and  $F_{fw}$  is slow, which makes optimizing the multi-dimensional parameter space challenging.

We present a computationally efficient algorithm, described in Table I, which optimizes the  $Q$  of a self-resonant structure while considering  $F_{cc}$  and  $F_{fw}$ . This algorithm is computationally efficient because it reduces a multi-dimensional optimization into 2-dimensions. The design variables are the number of sections  $m$ , closely related to  $h_w$ , and the height of the magnetic core back-plate  $h_{bp}$ . The total height of the structure  $h_s$  and the desired resonant frequency  $\omega_0$  are constrained.

The algorithm first estimates the inductance of the structure (step 1 in Table I). The exact inductance is unknown until the optimal values of  $h_{bp}$ ,  $h_w$  and  $h_{gap}$  are selected. Thus, as an initial guess for step 1, the inductance of the structure is estimated using magnetostatic finite element analysis (FEA) simulation assuming that  $h_{bp}$ ,  $h_w$  and  $h_{gap}$  are each approximately one third of  $h_s$ . Because the inductance of the structure is dominated by the reluctance path in the air, this approximation does not significantly impact the optimization results. In a practical design, there is some space between the bottom of the winding and the top of the core backplate due to the presence of the first layer, which is thick compared to the skin depth.

The estimated inductance is then used to calculate the losses in the structure for various combinations of  $m$  and  $h_{bp}$  (steps 2–6). The structure height constraint limits the possible combinations of  $m$  and  $h_{bp}$  that need to be considered since there exists a maximum number of sections  $m$  that can fit inside of the pot core for a particular value of  $h_{bp}$ . For each  $\{m, h_{bp}\}$  combination, the algorithm computes the estimated  $Q$  from the loss models in [1], [10]. First, the

TABLE I: Computationally efficient algorithm to produce a design-space for a thin self-resonant structure.

Description of Algorithm Steps	Tool/Equation
1) Estimate $L$	Magnetostatic FEA
2) Select $\{m, h_{bp}\}$ design space	None
<i>For each <math>\{m, h_{bp}\}</math> combination, do (3–6)</i>	
3) Estimate dielectric thickness	$t_d = \frac{\epsilon_0 k (r_2^2 - r_1^2) \theta m L \omega_0^2}{2\pi}$
4) Estimate conductor thickness	$t_c = \frac{3^{0.25} \delta}{\sqrt{m}} \left( \frac{k_1}{k_2} \right)^{\frac{1}{4}}$
5) Simulate lateral current crowding	FEA procedure in [1]
6) Calculate $Q$	$Q = \frac{\omega_0 L}{R_{total}}$
7) Find $\{m, h_{bp}\}$ for optimum $Q$ .	None
<i>For the optimal <math>\{m, h_{bp}\}</math> combination, do (8–12)</i>	
8) Calculate $t_c$ considering $F_{cc}$ and $F_{fw}$	$t_c = \frac{3^{0.25} \delta}{\sqrt{m}} \left( \frac{k_1 F_{cc}}{k_2 F_{fw}} \right)^{\frac{1}{4}}$
9) Calculate $L$ with updated $h_w$ and $h_{bp}$	Magnetostatic FEA
10) Update dielectric thickness	$t_d = \frac{\epsilon_0 k (r_2^2 - r_1^2) \theta m L \omega_0^2}{2\pi}$
11) Simulate lateral current crowding	FEA procedure in [1]
12) Unless $t_c$ has converged go to step 8	None

required dielectric thickness is

$$t_d = \frac{\epsilon_0 k (r_2^2 - r_1^2) \theta m L \omega_0^2}{2\pi}, \quad (10)$$

which is computed from (1), (2), and (3). The optimal conductor thickness, assuming no current crowding or field weakening, for a given number of sections is derived in [10], and is

$$t_c = \frac{3^{0.25} \delta}{\sqrt{m}} \left( \frac{k_1}{k_2} \right)^{\frac{1}{4}}. \quad (11)$$

Using the conductor thickness and dielectric thickness, a procedure, presented in [1], is used to compute  $F_{cc}$  and  $F_{fw}$ . Finally,  $Q$  is computed from  $L$ , (5), (7), and (9). The optimal  $\{m, h_{bp}\}$  combination that minimizes the total loss, hence maximizes  $Q$ , is then selected (step 7).

Once the optimal  $\{m, h_{bp}\}$  combination is selected, an iterative process is used to find more precise solutions for the dielectric thickness and the optimal conductor thickness (steps 8–12). The dielectric thickness is dependent on the inductance of the structure. A more accurate estimate of the structure's inductance is calculated using FEA based on the winding area and core shape obtained from the optimal  $\{m, h_{bp}\}$  combination. The optimal conductor thickness is dependent on lateral current crowding, so the conductor thickness is also reevaluated. The optimal conductor thickness including current crowding and field weakening  $t_{c,opt}$  is derived by minimizing the AC resistance factor  $F_r$

$$F_r = \frac{k_1 F_{cc}}{m t_c} + \frac{m}{9} \cdot \frac{t_c^3}{\delta^4} k_2 F_{fw} \quad (12)$$

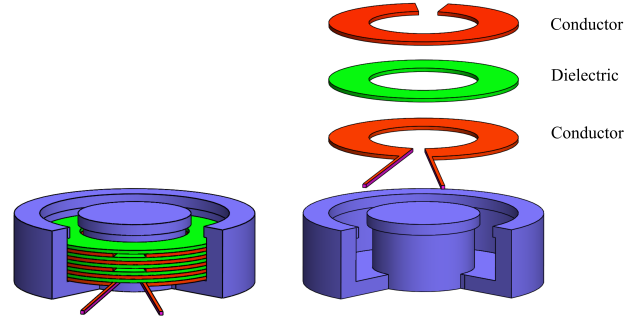


Fig. 4: A self-resonant structure in a modified pot core is shown. A few layers of the winding are expanded on the right to show the orientation of the conductive layers.

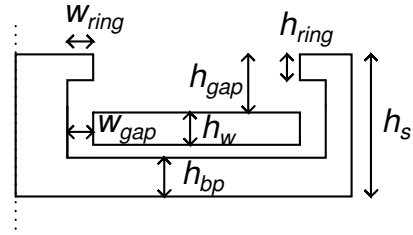


Fig. 5: A diagram of the modified pot core shape that is axissymmetric around the dotted line. This diagram is not to scale, but enlarged in order to clearly define: the winding height  $h_w$ , the magnetic core back-plate height  $h_{bp}$ , the width of the ring  $w_{ring}$ , the height of the ring  $h_{ring}$ , and the total height of the structure  $h_s$ .

with respect to the conductor thickness, and is

$$t_{c,opt} = 3^{0.25} \frac{\delta}{\sqrt{m}} \left( \frac{k_1 F_{cc}}{k_2 F_{fw}} \right)^{0.25}. \quad (13)$$

This process of calculating  $t_d$  and  $t_{c,opt}$  and performing FEA simulation to obtain  $F_{cc}$  and  $F_{fw}$  can be repeated in order to converge to a more precise solution. An example design space is shown in Fig. 6.

#### IV. MODIFIED POT CORE

In very thin structures with an ordinary pot core, lateral current crowding causes the winding loss to be much larger than in a deeper structure, even though it's still small compared to that of a conventional coil. To help overcome this, we propose a new core shape called the modified pot core. The modified pot core has two rings of magnetic core material that overhang the winding, as shown in Fig. 4. These additional rings of magnetic core material shape the magnetic field so that it is more parallel to the conductors, as can be seen by comparing Figs. 3b and 3c, and the more parallel magnetic field lines reduce lateral current crowding.

The width of the ring  $w_{ring}$  and the height of the ring  $h_{ring}$  (shown in Fig. 5) are important design parameters. Increasing the width of the ring until  $\frac{w_{ring}}{w_{gap}} \approx 1.5$  helps shape the magnetic field and increases the  $Q$  of the resonant structure, but it also slightly increases the leakage inductance, which slightly decreases the  $k$ . In general,  $w_{ring}$  should be about as large as the distance between the edge of the winding and the

edge of the pot core  $w_{gap}$ . The height of the ring impacts the available space for the winding, and therefore should be just large enough to be easily manufactured. The modified pot core provides up to a  $1.46\times$  increase in quality factor compared to the conventional pot core for the example shown in Section V.

## V. RESULTS

This section applies the tools discussed in Sections III and IV to the design of self-resonant structures with a resonant frequency of 6.78 MHz. The structures use a pot core made from Fair-Rite 67 Ni-Zn ferrite with an outer diameter of 6.6 cm, which can fit a winding with an outer radius  $r_2$  of 26.75 mm and an inner radius  $r_1$  of 14.6 mm. The conductive layers are copper, and the dielectric layers are PTFE (Teflon). A gap of 125  $\mu\text{m}$  is included between the bottom of the winding and the top of the core in order to leave space for the drive layer of the resonant structure. Further details about the structure are cataloged in Table II. The modeled performance of the self-resonant structures is compared to the modeled performance of a reference design. The reference design is a single-turn, single-layer copper winding thicker than a skin-depth with  $r_2 = 26.75$  mm and  $r_1 = 14.6$  mm, placed in the same 6.6 cm pot core. This winding is connected to a low-loss capacitor with a dissipation factor of  $5 \times 10^{-4}$ . This dissipation factor was chosen to model the losses of an extremely high- $Q$  capacitor, ATC800E series, at 6.78 MHz.

### A. Optimizing Thin Resonant Structures

1) *Typical Pot Core*: The algorithm in Section III was used to create a contour plot, shown in Fig. 6, which illustrates the impact of the design parameters  $\{m, h_{bp}\}$  on the  $Q$  of a 3.5 mm tall structure. The shape of Fig. 6 provides quantitative evidence regarding the design trade-offs described in Section II. For example, if too many sections are used ( $m > 12$ ), the  $Q$  of the structure decreases either because winding loss increases due to  $h_{gap}$  being small or core loss increases due to  $h_{bp}$  being small. The maximum  $Q$  is  $Q_{max} = 511$ , and is found by optimizing  $\{m, h_{bp}\}$  to minimize loss.

2) *Modified Pot Core*: A contour plot demonstrating the relationship between  $\{m, h_{bp}\}$  and  $Q$  is also shown for the self-resonant structure in a modified pot core. The total height of the structure is constrained to 3.5 mm, and the height of the ring  $h_{ring}$  is 500  $\mu\text{m}$ . The optimal  $w_{ring}$  is determined by considering  $Q$  and  $Q \cdot k$  as a function of  $\frac{w_{ring}}{w_{gap}}$ . In Fig. 7, the  $Q \cdot k$  and  $Q$  of a 3.5 mm self-resonant structure in a modified pot core are shown as a function of  $\frac{w_{ring}}{w_{gap}}$ . For this example, using the modified pot core in place of the conventional pot core can increase the  $Q$  of the self-resonant structure from 494 to 718 ( $\sim 1.45\times$  improvement). Thus, the benefit of the self-resonant structure relative to the reference design can be larger if the modified pot-core is used. Although the  $\frac{w_{ring}}{w_{gap}}$  that maximizes  $Q$  in Fig. 7 is approximately 2, inserting a winding into a core with  $\frac{w_{ring}}{w_{gap}} > 1$  is challenging because the winding is larger than the core opening. Therefore, the modified pot core is assumed to have  $\frac{w_{ring}}{w_{gap}} = 1$ .

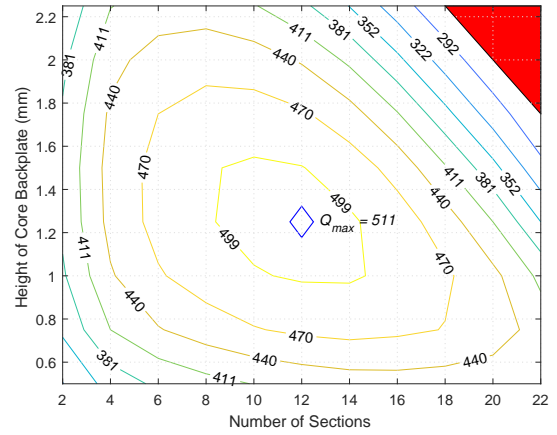


Fig. 6: The quality factor is plotted as a function of the number of sections  $m$  and the back-plate height  $h_{bp}$  for a 6.78 MHz self-resonant structure with a 3.5 mm high pot core. The blue diamond marks the maximum calculated  $Q$ , which is  $Q_{max} = 511$ . The red shaded area represents  $\{m, h_{bp}\}$  combinations in which the winding does not fit inside of the pot core.

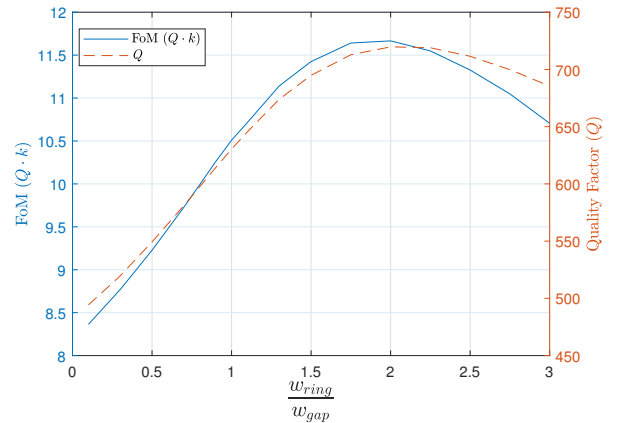


Fig. 7: Finite element analysis of a 3.5 mm modified pot core structure is used to plot the  $Q$  and  $\text{FoM } Q \cdot k$  for varying ring widths  $w_{ring}$  normalized to the winding gap  $w_{gap}$ . The magnetic coupling is computed using FEA of two structures separated by 66 mm.

The impact of  $\{m, h_{bp}\}$  on  $Q$  for the self-resonant structure with a 3.5 mm high modified pot core with  $h_{ring} = 0.5$  mm and  $\frac{w_{ring}}{w_{gap}} = 1$  is shown in Fig. 8. In this figure, designs that have a winding that is larger than the available winding space ( $h_w > h_s - h_{bp}$ ) are shaded in red. Designs that maximize the  $Q$  fully utilize the winding space, and therefore are adjacent to the red shaded area.

The contour plots for the two core shapes are qualitatively different. For the conventional pot core, there exists an optimal number of sections for each back-plate height as adding more sections reduces the gap between the top of the core and the top of the winding, which causes magnetic field lines to be less parallel to the conductor layers. The modified pot core significantly reduces the effect of this gap, and the optimal design for each back-plate height uses the maximum number of sections that can fit inside of the modified pot core such

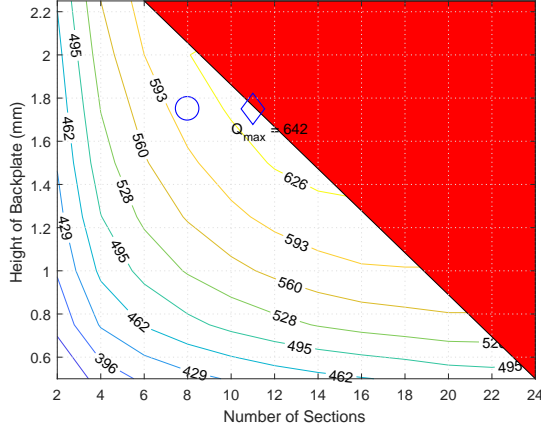


Fig. 8: The quality factor is plotted as a function of the number of sections  $m$  and the back-plate height  $h_{bp}$  for a 6.78 MHz self-resonant structure with a 3.5 mm high modified pot core with  $h_{ring} = 0.5$  mm and  $\frac{w_{ring}}{w_{gap}} = 1$ . In order to account for the thickness of the bottom driving layer, a gap of 0.125 mm between the bottom of the winding and the magnetic core back-plate is assumed in the simulation. The red shaded area represents  $\{m, h_{bp}\}$  combinations in which the winding does not fit inside of the modified pot core. The blue diamond indicates the  $\{m, h_{bp}\}$  that achieves  $Q_{max} = 642$ , and the blue circle indicates the design used in the experimental setup, which has an expected  $Q$  of 605.

that the top of the winding touches the bottom of the ring of the modified pot core.

3)  $Q$  vs. Structure Height: Contour plots are created for various structure heights  $h_s$  ranging from 2 mm to 6 mm to find the optimal  $\{m, h_{bp}\}$  that maximizes  $Q$  for each  $h_s$ . Fig. 9 shows the maximum quality factor  $Q_{max}$  as a function of the total structure height  $h_s$  for both the self-resonant structure and the self-resonant structure in a modified pot core. For comparison, the maximum  $Q$  theoretically achievable with a single-layer reference design is also included in Fig. 9. The self-resonant structure outperforms the reference design over the plotted range. Even with small structure heights, where the benefit is smaller, the resonant structure has a substantial advantage, especially with the modified pot core. Using the modified pot core, the self-resonant structure has a  $Q_{max}$   $1.90\times$  larger than the reference design at 6 mm, and  $1.52\times$  at 2 mm. Furthermore, the self resonant structure in a modified pot core has a  $Q$   $1.30\times$  larger than the self-resonant structure in a typical pot core at 2 mm.

### B. Experimental Validation

In order to experimentally validate the results in Fig. 9, we built a self-resonant structure optimized for  $h_s = 3.5$  mm, adjusting the optimal number of sections from 12 to 8 to make building the coil by hand feasible. The expected  $Q$  of this structure was 605.

The low loss dielectric layers were created from 12.5  $\mu\text{m}$  PTFE film cut into ring shapes with a die cutter. The optimal conductor thickness was found to be 12.1  $\mu\text{m}$ , so the conductive layers were created from 12.5  $\mu\text{m}$  thick copper foil cut into C-shapes with a die cutter. Substrate layers were used

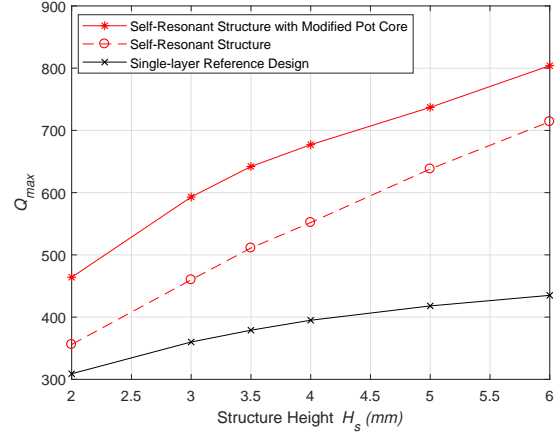


Fig. 9: This figure illustrates the impact of structure height on the  $Q_{max}$  of the self-resonant structure, self-resonant structure in a modified pot core, and the reference design.

TABLE II: Thin 3.5 mm self-resonant coil variables and values in the experimental setup.

Parameter	Description	Value
$f_o$	Desired resonant frequency	6.78 MHz
$t_c$	Conductor thickness	12.5 $\mu\text{m}$
$t_d$	Dielectric thickness	12.5 $\mu\text{m}$
$k$	Dielectric constant	2.2
$D_f$	Dissipation factor	$3 \times 10^{-4}$
$m$	Number of sections	8
$\theta$	Overlap angle	$\sim 175^\circ$
$r_2$	Conductor outer radius	26.75 mm
$r_1$	Conductor inner radius	14.6 mm
$w_{gap}$	Conductor inner radius	0.5 mm
$\delta$	Skin Depth	25 $\mu\text{m}$
$\rho$	Conductor resistivity	16.8 n $\Omega$ -m
$\mu'$	Core permeability	40 $\mu_0$
$\mu''$	Imaginary permeability	0.7 $\mu_0$

to support the thin layers in [1], which added to the overall winding height. In order to reduce the winding height, we developed a working prototype without any substrate layers. We eliminated wrinkling from handling and cutting the copper layers by pressing them in a vice between two 1 cm thick polypropylene blocks. The resonant coil was built into the modified pot core, as shown in Fig. 10.

Experimental results were obtained by testing the coil in the 3.5 mm modified pot core. The  $Q$  of the structure was obtained by measuring the structure's impedance as a function of frequency using an Agilent 4294A impedance analyzer. The resonant frequency  $f_0$  was divided by the -3dB bandwidth  $\Delta f_{3dB}$  to give  $Q = \frac{f_o}{\Delta f_{3dB}}$ . The measured  $Q$  of the modified structure was 560, giving a  $Q_d$  of 84.8. There was 7.4% error between our predicted and experimental results. This demonstrates the accuracy of our modeling and the high performance of the modified structure.

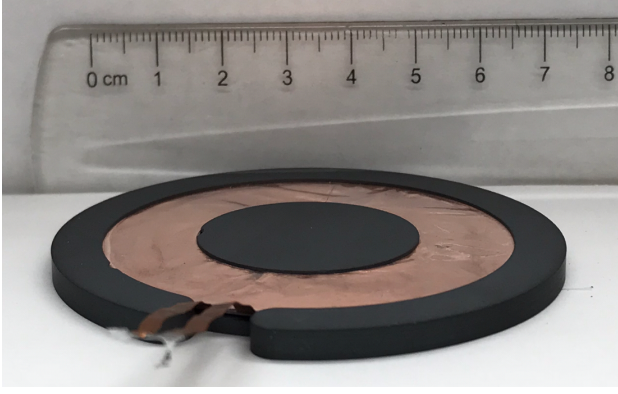


Fig. 10: The modified structure consists of the self-resonant coil built into the 3.5 mm tall modified pot core.

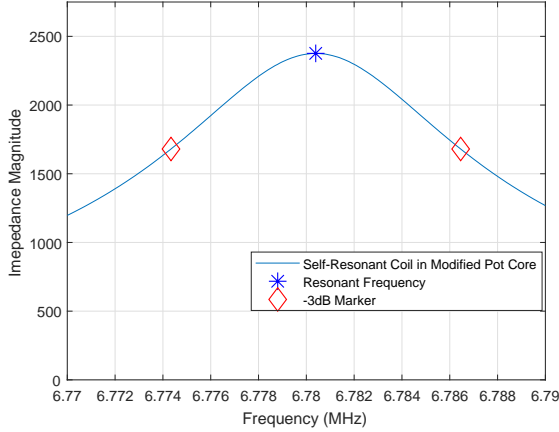


Fig. 11: Measured impedance of the self-resonant structure as described in Table II. The quality factor of the resonance is calculated from the resonance frequency and the -3 dB bandwidth.

### C. Impact on Wireless Power Transfer

The high- $Q$  of the experimental self-resonant structure in a modified pot core allows for high efficiency and longer range WPT. The maximum achievable WPT efficiency as a function of  $Q$  and  $k$  is

$$\eta_{max} = \frac{(Qk)^2}{\left(1 + \sqrt{1 + (Qk)^2}\right)^2}. \quad (14)$$

The expected  $\eta_{max}$  for both our experimental self-resonant structure and the current state of the art is shown in Fig. 12. The  $\eta_{max}$  of our experimental self-resonant structure is based on the experimental  $Q$  of 560 and the  $k$  of the modified pot core is calculated using FEA. The  $\eta_{max}$  of the state-of-the-art is based on the expected  $Q_{soa}$  of a 6.6 cm state-of-the-art coil, which is  $Q_{soa} = Q_d \cdot d = 184.4$ , and  $k$  is estimated using FEA of a typical 3.5 mm thick pot core with a diameter of 6.6 cm.

The experimental self-resonant structure significantly outperformed the state-of-the-art design. It was able to achieve above 90% efficiency over a range of 48.5 mm, which is a 56% increase over that of the state-of-the-art. Furthermore, at

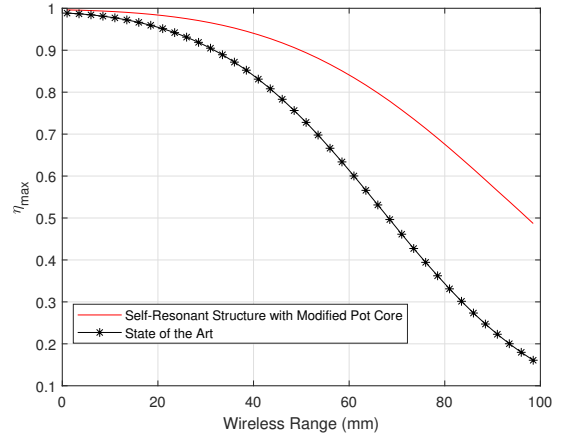


Fig. 12: Maximum wireless power transfer efficiency as a function of the wireless range. The  $\eta_{max}$  of our experimental self-resonant structure is based on the experimental  $Q$  of 560 and a simulated  $k$ , which is computed using FEA of a 3.5 mm modified pot core. The  $\eta_{max}$  of the state-of-the-art is based on the expected  $Q_{soa}$  of 184, and a simulated  $k$ , which is estimated using FEA of a typical 3.5 mm thick pot core.

TABLE III: The FoM, described in [11], is calculated for a sample of WPT systems utilizing various resonant coil technologies in the literature and are catalogued below.

Citation	Frequency	Coil Technology	Max FoM
[7]	7.65 MHz	Solid wire coil	0.11
[12]	15.9 MHz	Solid wire coil	0.61
[6]	10.6 MHz	Solid wire coil	0.97
[8]	3.7 MHz	Surface spiral coil	0.34
[13]	50 kHz	Litz wire coil	0.52
This Work	6.78 MHz	Self-Resonant Structure	3.38

60 mm the self-resonant structure has  $2.5\times$  lower loss.

A figure of merit for resonant wireless power transfer FoM is described in [11], and can be used to describe the relative performance of a WPT systems. Using  $\eta_{max}$ , the FoM is computed and plotted in Fig. 13 for our experimental structure and systems from the literature, which are described in Table III. The other reported systems are not designed to be thin, so this plot compares the performance of our structure against coils that could be much thicker.

The self-resonant structure significantly outperforms other systems in the literature when the range/diameter is  $\frac{x}{d} < 1.25$ . The maximum FoM is 3.38, which is  $\sim 6\times$  larger than other systems that report data for  $\frac{x}{d} < 1.25$ , despite being only 3.5 mm thick. As the range increases (i.e.  $\frac{x}{d} > 1.25$ ), the FoM of our structure approaches that of [6]. The resonant coil presented in [6] does not have a magnetic core, so the magnetic coupling factor is relatively large at long range.

## VI. CONCLUSIONS AND FUTURE WORK

Many wireless power transfer application require very thin yet high- $Q$  resonant coils. In this work, we explore the relationship between the  $Q$  of self-resonant structures and their thickness. We propose a computationally efficient algorithm

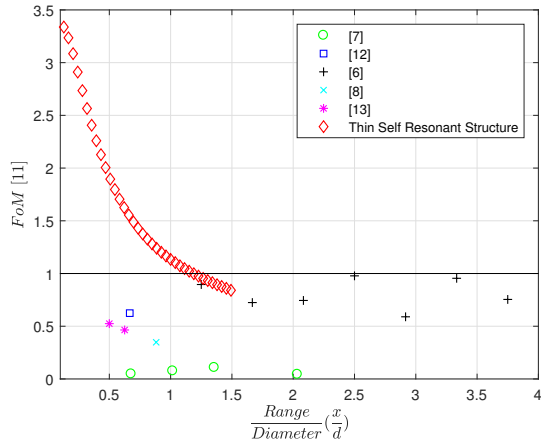


Fig. 13: Figure of merit, described in [11], as a function of  $\frac{\text{range}}{\text{diameter}}$  is shown for our thin self-resonant structure in a modified pot core and a few examples from the literature.

for computing a 2-dimensional design space for thin high- $Q$  self-resonant structures and introduces a new core shape which drastically reduces winding loss in thin structures. Simulation results show that the self-resonant structure can achieve a  $Q$  more than  $1.5\times$  larger than a single layer design for structures that thicker than 2 mm. An experimental implementation of 3.5 mm thick self-resonant structure in a modified pot core validates our simulation results, and demonstrates that thin self-resonant structures can achieve high  $Q$ . This work highlights how self-resonant structure can be used to increase the range and efficiency of WPT in applications which limit the available thickness.

Future work on self-resonant structures will consider magnetic coupling  $k$  as part of the structure optimization, in order to further extend the range of wireless power transfer.

#### ACKNOWLEDGMENTS

This material is based upon work supported by the National Science Foundation under Grant No. 1507773.

#### REFERENCES

- [1] A. L. F. Stein, P. A. Kyaw, and C. R. Sullivan, "High- $Q$  self-resonant structure for wireless power transfer," in *Applied Power Electronics Conference and Exposition (APEC)*. IEEE, 2017.
- [2] C. R. Sullivan, B. A. Reese, A. L. F. Stein, and P. A. Kyaw, "On size and magnetics: Why small efficient power inductors are rare," in *International Symposium on 3D Power Electronics Integration and Manufacturing (3D-PEIM)*. IEEE, 2016, pp. 1–23.
- [3] K. Fotopoulou and B. W. Flynn, "Wireless power transfer in loosely coupled links: Coil misalignment model," *Transactions on Magnetics*, vol. 47, no. 2, pp. 416–430, 2011.
- [4] C. Florian, F. Mastri, R. P. Paganelli, D. Masotti, and A. Costanzo, "Theoretical and numerical design of a wireless power transmission link with GaN-based transmitter and adaptive receiver," *Transactions on Microwave Theory and Techniques*.
- [5] A. Khripkov, W. Hong, and K. Pavlov, "Design of an integrated resonant structure for wireless power transfer and data telemetry," in *Microwave Workshop Series on RF and Wireless Technologies for Biomedical and Healthcare Applications (IMWS-BIO)*. IEEE, 2013, pp. 1–3.
- [6] A. Kurs, A. Karalis, R. Moffatt, J. D. Joannopoulos, P. Fisher, and M. Soljačić, "Wireless power transfer via strongly coupled magnetic resonances," *Science*, vol. 317, no. 5834, pp. 83–86, 2007.
- [7] A. P. Sample, D. A. Meyer, and J. R. Smith, "Analysis, experimental results, and range adaptation of magnetically coupled resonators for wireless power transfer," *Transactions on Industrial Electronics*, vol. 58, no. 2, pp. 544–554, 2011.
- [8] S.-H. Lee and R. D. Lorenz, "Development and validation of model for 95%-efficiency 220 watt wireless power transfer over a 30-cm air gap," *Transactions on Industry Applications*, vol. 47, no. 6, pp. 2495–2504, 2011.
- [9] C. R. Sullivan, "Cost-constrained selection of strand diameter and number in a litz-wire transformer winding," *Transactions on Power Electronics*, vol. 16, no. 2, pp. 281–288, 2001.
- [10] C. R. Sullivan and L. Beghou, "Design methodology for a high- $Q$  self-resonant coil for medical and wireless-power applications," in *14th Workshop on Control and Modeling for Power Electronics (COMPEL)*. IEEE, 2013, pp. 1–8.
- [11] A. L. Stein, P. A. Kyaw, and C. R. Sullivan, "Figure of merit for resonant wireless power transfer," in *Control and Modeling for Power Electronics (COMPEL)*. IEEE, 2017, pp. 1–7.
- [12] T. Imura, H. Okabe, and Y. Hori, "Basic experimental study on helical antennas of wireless power transfer for electric vehicles by using magnetic resonant couplings," in *Vehicle Power and Propulsion Conference*. IEEE, 2009, pp. 936–940.
- [13] H. Takanashi, Y. Sato, Y. Kaneko, S. Abe, and T. Yasuda, "A large air gap 3 kW wireless power transfer system for electric vehicles," in *Energy Conversion Congress and Exposition (ECCE)*. IEEE, 2012, pp. 269–274.